Regulatory T Cells Recruited through CCL22/CCR4 Are Selectively Activated in Lymphoid Infiltrates Surrounding Primary Breast Tumors and Lead to an Adverse Clinical Outcome

Michael Gobert,[1,2,3,4] Isabelle Treilleux,[5] Nathalie Bendriss-Vermare,[1,2,3,4] Thomas Bachelot,[1,8] Sophie Goddard-Leon,[5] Vanessa Arfi,[1,2,3,4] Cathy Biota,[1,2,3,4] Anne Claire Doffin,[1,2,3,4] Isabelle Durand,[1,2,3,4] Daniel Olive,[7] Solène Perez,[8] Nicolas Pasqual,[8] Christelle Faure,[6] Isabelle Ray-Coquard,[6] Alain Puisieux,[1,2,3,4] Christophe Caux,[1,2,3,4] Jean-Yves Blay,[1,2,3,4] and Christine Ménétrier-Caux[1,2,3,4]

[1]INSERM, U590; [2]Centre Léon Bérard, Equipe Cytokines et Cancers; [3]Université Lyon 1, ISPB; [4]IFR62; [5]Centre Léon Bérard, Département D'anatomie et Cytologie Pathologiques; [6]Centre Léon Bérard, Département d'Oncologie Médicale, Lyon, France; [7]Laboratoire d'Immunologie des Tumeurs et Centre INSERM de Recherche en Cancérologie de Marseille, Institut Paoli Calmettes, Marseille, France; and [8]ImmunID Technologies, Grenoble, France

Abstract

Immunohistochemical analysis of FOXP3 in primary breast tumors showed that a high number of tumor-infiltrating regulatory T cells (Ti-Treg) within lymphoid infiltrates surrounding the tumor was predictive of relapse and death, in contrast to those present within the tumor bed. *Ex vivo* analysis showed that these tumor-infiltrating FOXP3$^+$ T cells are typical Treg based on their CD4$^+$CD25^{high}CD127^{low}FOXP3$^+$ phenotype, their anergic state on *in vitro* stimulation, and their suppressive functions. These Ti-Treg could be selectively recruited through CCR4 as illustrated by (*a*) selective blood Treg CCR4 expression and migration to CCR4 ligands, (*b*) CCR4 down-regulation on Ti-Treg, and (*c*) correlation between Ti-Treg in lymphoid infiltrates and intratumoral CCL22 expression. Importantly, in contrast to other T cells, Ti-Treg are selectively activated locally and proliferate *in situ*, showing T-cell receptor engagement and suggesting specific recognition of tumor-associated antigens (TAA). Immunohistochemical stainings for ICOS, Ki67, and DC-LAMP show that Ti-Treg were close to mature DC-LAMP$^+$ dendritic cells (DC) in lymphoid infiltrates but not in tumor bed and were activated and proliferating. Furthermore, proximity between Ti-Treg, CD3$^+$, and CD8$^+$ T cells was documented within lymphoid infiltrates. Altogether, these results show that Treg are selectively recruited within lymphoid infiltrates and activated by mature DC likely through TAA presentation, resulting in the prevention of effector T-cell activation, immune escape, and ultimately tumor progression. This study sheds new light on Treg physiology and validates CCR4/CCL22 and ICOS as therapeutic targets in breast tumors, which represent a major health problem. [Cancer Res 2009;69(5):2000–9]

Introduction

Cancer immunosubversion is a process (1) by which tumor cells escape destruction by the immune system through a variety of mechanisms. We previously described the production of interleukin (IL)-10 by intratumoral macrophages in renal cell carcinoma (2) and the alteration of dendritic cell (DC) differentiation by cytokines produced by renal and breast carcinomas (BC; refs. 3, 4). Other mechanisms have been described, among which the attraction of suppressive cells, particularly CD4$^+$CD25$^+$ regulatory T cells (Treg), a lymphocyte counterpart with immunoregulatory properties (see ref. 5 for review).

Several studies have shown that the immune system is present and functional against the tumor in BC patients and may promote both humoral and cellular responses (6, 7). The bone marrow of BC patients contains functional memory CD8$^+$ T cells specific for MUC-1 or HER2/neu proteins, suggesting a specific cellular response (8). In addition, different DC subpopulations infiltrate breast tumors, such as immature and mature myeloid DC (mDC), the latter being confined to the periphery of the tumor (4, 6, 9). BC blocks mDC maturation and functionality *in vitro* (4). Plasmacytoid DCs (see ref. 10 for review) also infiltrate primary BCs and their presence correlates with an adverse outcome (9). These results show that the presence of immune cells in breast tumors is unable to counteract cancer and may even contribute to tumor progression.

The role of Treg in immune evasion remains unclear. The number of Treg is increased in the peripheral blood of BC patients (11–13) and they are present within the primary tumors (11). Their effect on tumor progression vary according to the tumor type in humans: Treg have a negative effect on survival in pancreatic, liver, or ovarian carcinoma patients (14–16), whereas they may exert a beneficial role in follicular lymphoma (17) or head and neck carcinoma (18) or have no effect on survival (anal squamous cell carcinoma; ref. 19). Recently, two studies reported a negative effect of FOXP3$^+$ Treg in BC patient outcome (20, 21).

In the present study, we show from a prospectively collected cohort of BC patients with 8-year clinical follow-up that the topography of Treg in the stroma or at the immediate contact of tumor cells influences the outcome of these patients: the presence of FOXP3$^+$ Treg in lymphoid infiltrates surrounding the tumor mass identifies a subset of patients with increased risk of relapse and death, whereas those in the tumor area do not correlate to relapse-free survival (RFS) or overall survival (OS). We also show that functionally suppressive CD4$^+$CD25^{high}FOXP3$^+$ tumor-infiltrating Treg (Ti-Treg) contained in the lymphoid infiltrates of primary breast tumors display a highly activated phenotype that could be induced through DC-LAMP$^+$ DC interaction, showing *in situ* ongoing reactivity that dominates the tumor environment.

Note: Supplementary data for this article are available at Cancer Research Online (http://cancerres.aacrjournals.org/).

Requests for reprints: Christine Ménétrier-Caux, Centre Léon Bérard, Equipe Cytokines et Cancers, INSERM, U590, Lyon F-69008, France. Phone: 33-4-78-78-27-20; Fax: 33-4-78-78-27-50; E-mail: caux@lyon.fnclcc.fr.

doi:10.1158/0008-5472.CAN-08-2360

Furthermore, we show that this infiltration derives from specific Ti-Treg recruitment, probably through CCL22, one of the CCR4 ligand, and active proliferation at the tumor site.

Materials and Methods

Patient selection. The patients' selection for cellular biology and for the retrospective immunohistochemical study as well as the treatments used in the retrospective study are detailed in Supplementary Materials and Methods.

Immunohistochemical analysis. Stainings using HER2/neu (22), estrogen receptor (ER), and progesterone receptor (PgR) antibodies as well as CD3 and CD208/DC-LAMP (9) were carried out on tissue microarray (TMA) paraffin sections as previously described. CCL22 and FOXP3 stainings were performed using mouse anti-FOXP3 and goat anti-CCL22 (Supplementary Table S1), revealed with biotinylated secondary antibody bound to streptavidin peroxidase conjugate (LSAB$^+$ kit, Dako), and revealed with 3,3′-diaminobenzidine (DAB; Dako) as substrate. Hematoxylin-counterstained sections were analyzed independently by two pathologists according to the guidelines for HER2/neu amplification and ER/PgR positivity (22). CD3, CD208/DC-LAMP, or CCL22 was studied by semiquantitative analysis on 114, 108, and 161 patients, respectively. FOXP3$^+$ cells were enumerated using the ARIOL system (Applied Imaging). No linear dose response was observed between the absolute infiltration with FOXP3 cells: when introduced as numerical value, the number of FOXP3$^+$ cells was not retained in the model (data not shown). To compare the role of high number of FOXP3$^+$, we chose as cutoff the highest quartile (≥28 in lymphoid area and ≥18 in tumor area).

Double stainings on frozen sections. Frozen BC tissue sections from 20 patients were stained with mouse anti-FOXP3 or anti-Ki67 (Supplementary Table S1) and revealed using the ImmPRESS anti-mouse Ig peroxidase kit (Abcys) according to the supplier's instructions and DAB. Then, the second primary antibody (mouse anti-ICOS, anti-CD3, anti-CD8, anti-DC-LAMP, or anti-cytokeratin; Supplementary Table S1) was added and revealed with ImmPRESS kit and Histogreen (Abcys). The goat anti-CCL17 and anti-CCL22 (Supplementary Table S1) were revealed using biotinylated secondary antibody (Abcys) followed by extravidin peroxidase conjugate (Dako) and Histogreen revelation. The specificity of the staining was assessed using mouse or goat isotype controls in place of the first or the second primary antibody.

Enzymatic digestion of tumor tissue. A section of the resected tumor area selected by the pathologist was placed in RPMI 1640 with penicillin (100 IU/mL) and streptomycin (100 μg/L; Invitrogen). After mechanical

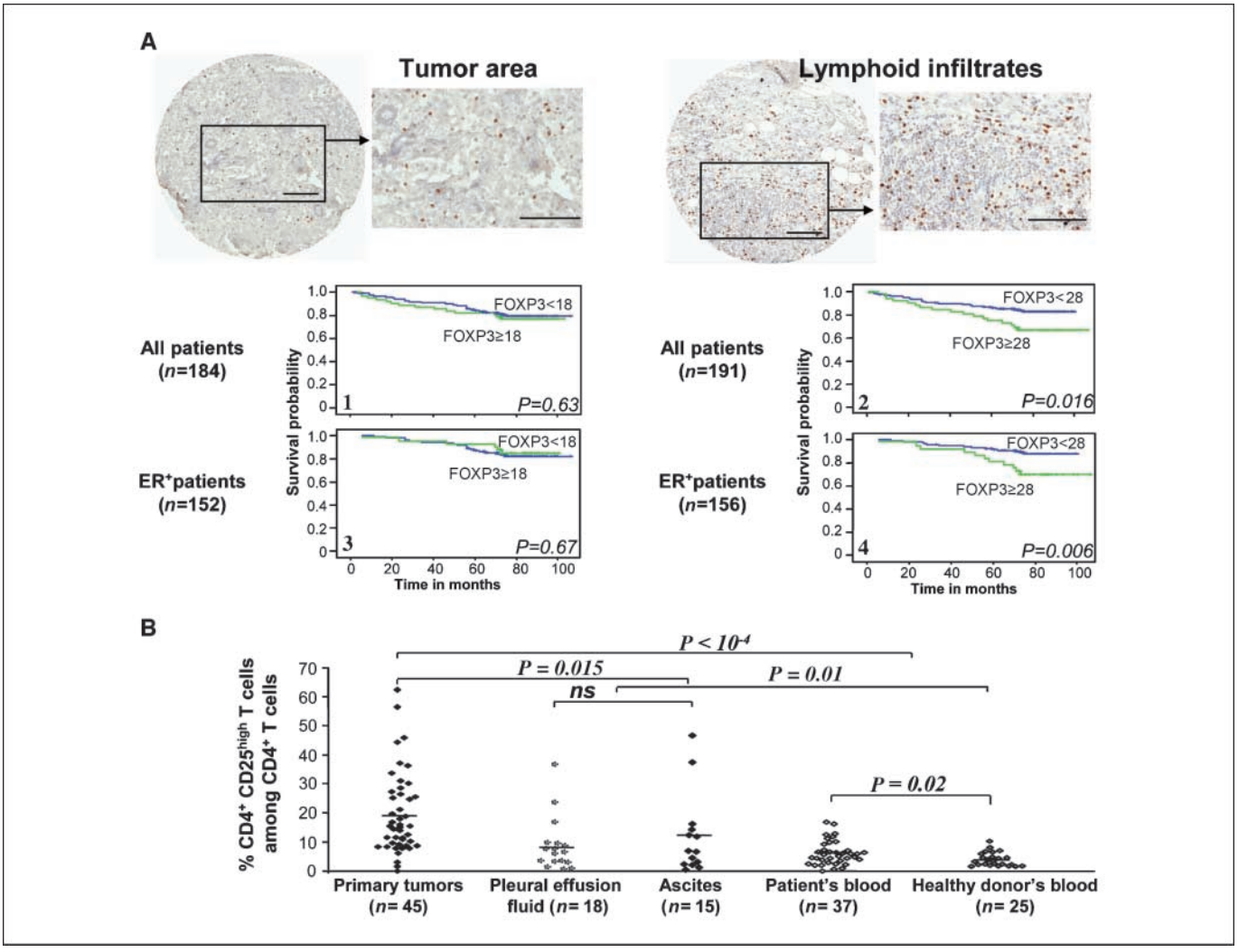

Figure 1. Treg accumulate in the primary tumor area: their presence within lymphoid infiltrates surrounding the tumor is associated with a higher risk of death. *A,* Treg were detectable in the tumor mass (*left*) or the lymphoid infiltrates (*right*) within the tumor using FOXP3 mAb (236AE/7). *Bars,* 100 μm. *1* to *4,* Kaplan-Meier curves for OS stratified according to the highest quartile value of FOXP3$^+$ Treg in the tumor area (cutoff ≥18; <18 = 138; ≥18 = 46; *1*) or lymphoid infiltrates (cutoff ≥28; <28 = 143; ≥28 = 48; *2*). Patients were further stratified according to their ER$^+$ status (*3, n* = 152; *4, n* = 156). *B,* percentages of CD4$^+$CD25^{high} cells among CD4$^+$ T cells were measured in the different biological samples (—, mean). Student's unpaired *t* test was performed on the means.

dilaceration, tumors were digested for 1 h at 37°C with collagenase Ia (1 μg/mL) and DNase I (50 kilounits/mL; Sigma) in medium with antibiotics and then resuspended in RPMI 1640 supplemented with 10% FCS (cRPMI) for further analyses.

Blood samples. Healthy human blood obtained anonymously from the "Etablissement Français du Sang" (Lyon, France) after donor informed consent was collected in sterile bags containing CTAD. Peripheral blood mononuclear cells (PBMC) were isolated by centrifugation on Pancoll (Dominique Dutscher). Cells were washed twice in PBS and diluted in cRPMI for further analyses.

Treg and conventional T-cell purification. $CD4^+CD25^-$ (Tconv) cells and $CD4^+CD127^{low}CD25^{high}$ Treg cells were purified from patients' primary tumors or effusions using either a cell sorter (FACSVantage SE flow cytometer, BD Biosciences) or a positive selection kit (Invitrogen) according to the supplier's instructions after $CD4^+$ T-cell prepurification. Purity was routinely >97% (n = 7, 97–99%) for $CD4^+CD25^{high}$ T cells and >94% for Tconv cells (n = 7, 94–97%).

Flow cytometry analysis. Triple staining by flow cytometry was performed on a FACScan (BD Biosciences) using monoclonal antibodies (mAb; Supplementary Table S2) or isotype-matched controls.

Intracellular FOXP3 (using either PHC101 or 259D FOXP3 clones) and CTLA-4 stainings were achieved in their specific FOXP3 Staining Buffer Set according to the supplier's protocol. We analyzed 20,000 events/condition on the total cell population using CellQuest Pro software (BD Biosciences) and 5,000 on purified cells.

Treg *in situ* proliferation analysis. The percentage of cycling Treg in primary breast tumors or paired blood was assessed by Ki67 or Hoechst 33342 staining. Cells were first double stained with cell membrane antibodies (CD25-PE/CD4-PE-Cy5) or specific isotype-matched controls to isolate Treg, and then Ki67-FITC staining was performed using the IntraStain kit (Dako) according to the supplier's protocol. Twenty thousand events/condition gated on $CD4^+$ cells were collected and analyzed.

After incorporation of Hoechst 33342 dye (Molecular Probes, Invitrogen) and triple cell surface staining (CD127/CD25/CD4) to discriminate Treg from Tconv, cells were analyzed on FACSVantage SE at 350 nm (UV, 45 mW) and the resultant fluorescence was measured at 424 nm. Cell doublets were excluded from the analysis recording width and area values of the fluorescence signal.

Immunosuppression assay. Purified Treg or Tconv cells (2.5×10^4 per well) were cultured in triplicate with anti–CD3/CD28-coated beads (one bead for 10 T cells; Invitrogen) or with allogeneic monocyte-derived DC (one monocyte-derived DC for 10 T cells) in 96-well round-bottom plates in cRPMI 1640. Tconv cells (2.5×10^4) were cocultured in triplicate with autologous purified Treg at a ratio of 1:1, 5:1, or 10:1. [^{3}H]Thymidine (Amersham) was added on day 4 for 18 h (0.5 μCi/well), and then cells were harvested and counted in a Betaplate scintillation counter (Perkin-Elmer).

Migration. The migration of healthy Treg obtained after 3 wk of expansion in the presence of anti–CD3/CD28-coated beads (Invitrogen) and high recombinant human IL-2 concentrations (Proleukin, Novartis; ref. 23) was performed as previously described (24).

ELISA. Cytokines (IL-2, IFN-γ, and IL-10; Bender Medsystems, Tebu-Bio) or chemokines (CCL22 and CCL17; R&D) were detected by ELISA. Detection thresholds were, respectively, 3.9, 7.6, and 3.1 pg/mL for cytokines and 7.8 pg/mL for both chemokines.

Statistical analyses. All statistical analyses were done using the Statistical Package for the Social Sciences 12.0 package (SPSS software). Correlations between clinicobiological data and the $FOXP3^+$ Treg content in the lymphoid infiltrates or tumor area were determined using a χ^2 test. Means of Treg content in blood and metastatic or primary tumors and activation status of Ti-Treg were compared using Student's t test or the nonparametric Wilcoxon test. Percentages or mean fluorescence intensity (MFI) expression of specific markers on Tconv and Treg was compared using the nonparametric Wilcoxon test. Survival curves were plotted using the Kaplan-Meier method and compared using the log-rank test. Multivariate analyses of prognostic factors for survival were performed using Cox model. A logistic regression model was used to identify independent variables correlated to Treg infiltration.

Results

The presence of $FOXP3^+$ Treg within lymphoid infiltrates surrounding the tumor is associated with a higher risk of relapse and death. $FOXP3^+$ Treg are detectable in breast tumors (20, 21). We performed immunohistochemical analysis with FOXP3 mAb on formalin-fixed tumor TMA cores specific for tumor area or lymphoid infiltrates (n = 191). High numbers (the highest quartile defined as cutoff) of $FOXP3^+$ Treg were detectable either in the tumor bed (FOXP3 ≥ 18 = 46; FOXP3 < 18 = 138) or in lymphoid aggregates (FOXP3 ≥ 28 = 48; FOXP3 < 28 = 143; Fig. 1*A*). The presence of $FOXP3^+$ Treg in the lymphoid infiltrates or within the tumor area was significantly correlated with high Scarff-Bloom-Richardson (SBR) histologic grade (25), HER2/neu amplification, and lack of ER/PgR expression (Supplementary Table S3), whereas no correlation was found with lymph node or tumor size involvement. Using linear regression analysis, HER2/neu-amplified tumors (P = 0.002) and ER expression (P = 0.015) were found independently correlated to the number of $FOXP3^+$ Treg in lymphoid aggregates.

Importantly, the presence of $FOXP3^+$ Treg in lymphoid-enriched areas was associated in univariate analysis with a higher risk of relapse with a shorter RFS (P = 0.025; data not shown) and OS (P = 0.016; Fig. 1*A, 2*), whereas the presence of $FOXP3^+$ cells in the tumor bed did not correlate to OS (P = 0.63; Fig. 1*A, 1*). This observation was even strengthened in the ER^+ subgroup [RFS, P = 0.006 (data not shown); OS, P = 0.009 (Fig. 1*A, 3* and *4*)] or when eliminating from the analysis triple-negative patients (13.3%) assessed to be of the worst prognosis (ref. 26) [RFS, P = 0.0033; OS, P = 0.0019 (data not shown)].

Using Cox model, introducing tumor size, number of involved lymph nodes, ER, PgR expression, and SBR grading, FOXP3 expression in lymphoid infiltrates was found to be an independent prognostic factor for OS [FOXP3 relative risk (RR), 2.24; P = 0.028], along with the SBR grading (RR, 4.39; $P < 10^{-4}$) and the tumor size (RR, 1.56; P = 0.006). Similar data were obtained for RFS (FOXP3 RR, 2.16; P = 0.043).

$CD4^+CD25^{high}$ Treg accumulate within breast tumors. The analysis of breast tumors showed that T cells were the main leukocyte-infiltrating population identified in freshly disaggregated primary BC infiltrates (mean, 61.6%; range, 16–88) and in pleural or ascitic fluids (mean, 52.1%; range, 9–89; Supplementary Fig. S1).

In primary tumors, Treg detected by $CD25^{high}$ (MFI > 10^2), FOXP3 expression, and low or no expression of CD127 (Supplementary Fig. S2*A*; ref. 27) represented 27.9% of $CD4^+$ T cells (range, 1.5–62.1%; Supplementary Figs. S1*B* and S3). The Treg content was also increased in breast metastatic ascites [n = 15, 12% (0.4–47.3)] and pleural effusions [n = 18, 8.3% (0.3–36.8; P = 0.01)] and in the peripheral blood of BC patients [6.12% (0.02–16.7; P = 0.02)] compared with healthy donors' peripheral blood Treg content [3.98% (1.1–5.2); Supplementary Fig. S1*B* and Fig. S3].

Purified Treg from primary BC exert suppressive functions *in vitro*. The purification of Ti-Treg from primary tumors or ascitic fluids (data not shown) yielded from 96% to 99% pure $CD4^+CD25^{high}$ T cells expressing intranuclear FOXP3 (Supplementary Fig. S4*A*), whereas Tconv cells were negative for FOXP3. As expected, on activation, purified Ti-Treg or those from ascitic fluids (data not shown) did not proliferate nor produce cytokines and block the proliferation of autologous Tconv cells stimulated with anti–CD3/CD28-coated beads or allogeneic $DC\text{-}LAMP^+$ monocyte-derived DC (data not shown). In addition, IL-2 and

IFN-γ (Supplementary Fig. S4*C* and *D*) production in the supernatant strongly decreased in the presence of Ti-Treg.

Ti-Treg are selectively recruited in primary tumors probably through CCL22/CCR4. By comparing T lymphocyte subsets infiltrating primary tumors and those of matched peripheral blood, we observed a strong increase ($P = 0.003$) in $CD4^+CD45RO^+$ memory T cells (98.3% compared with 35%; Supplementary Fig. S5*A* and *B*) and in Treg frequency (7.1% of $CD3^+$ T cells in primary tumors versus 1.9% in paired blood; $P = 0.002$; Supplementary Fig. S5*A* and *C*).

The phenotype of Tconv cells and Ti-Treg was compared with that of matched or healthy peripheral blood without purification after gating on $CD4^+FOXP3^-$ and $CD4^+FOXP3^+$ cells using PHC101 (Fig. 2*A*) or 259D (data not shown) FOXP3 clones.

The expression of CD62L, involved in the homing into lymph nodes, was strongly reduced in Ti-Treg compared with patient blood Treg. Furthermore, levels of CD62L were lower in circulating Treg from patients compared with normal donors, suggesting overall higher frequency of experienced Treg in patients' blood. Whereas CCR7 (CCL19 and CCL21 receptor) was expressed on both Tconv and Treg from blood (Fig. 2*A*), only circulating Treg expressed CCR4 [CCL17 and CCL22 receptor (28); 77%, MFI = 72; Fig. 2*A*; Supplementary Fig. S6]. In contrast to CXCR4 expression (CXCL12 receptor; data not shown), CCR4 and CCR7 were strongly down-regulated on Ti-Treg (MFI = 20; $P = 0.008$ for CCR4 and $P < 10^{-4}$ for CCR7 at MFI levels; Fig. 2*A*; Supplementary Fig. S6). Like freshly isolated Treg, *in vitro*–expanded Treg from healthy donors were capable of migrating in response to recombinant human CCL22 (rhCCL22) and recombinant human CCL17 (rhCCL17; Fig. 2*C*). Both *ex vivo*–purified healthy blood Treg (data not shown) and expanded Treg decreased their CCR4 expression, without CXCR4 modulation, through an active mechanism

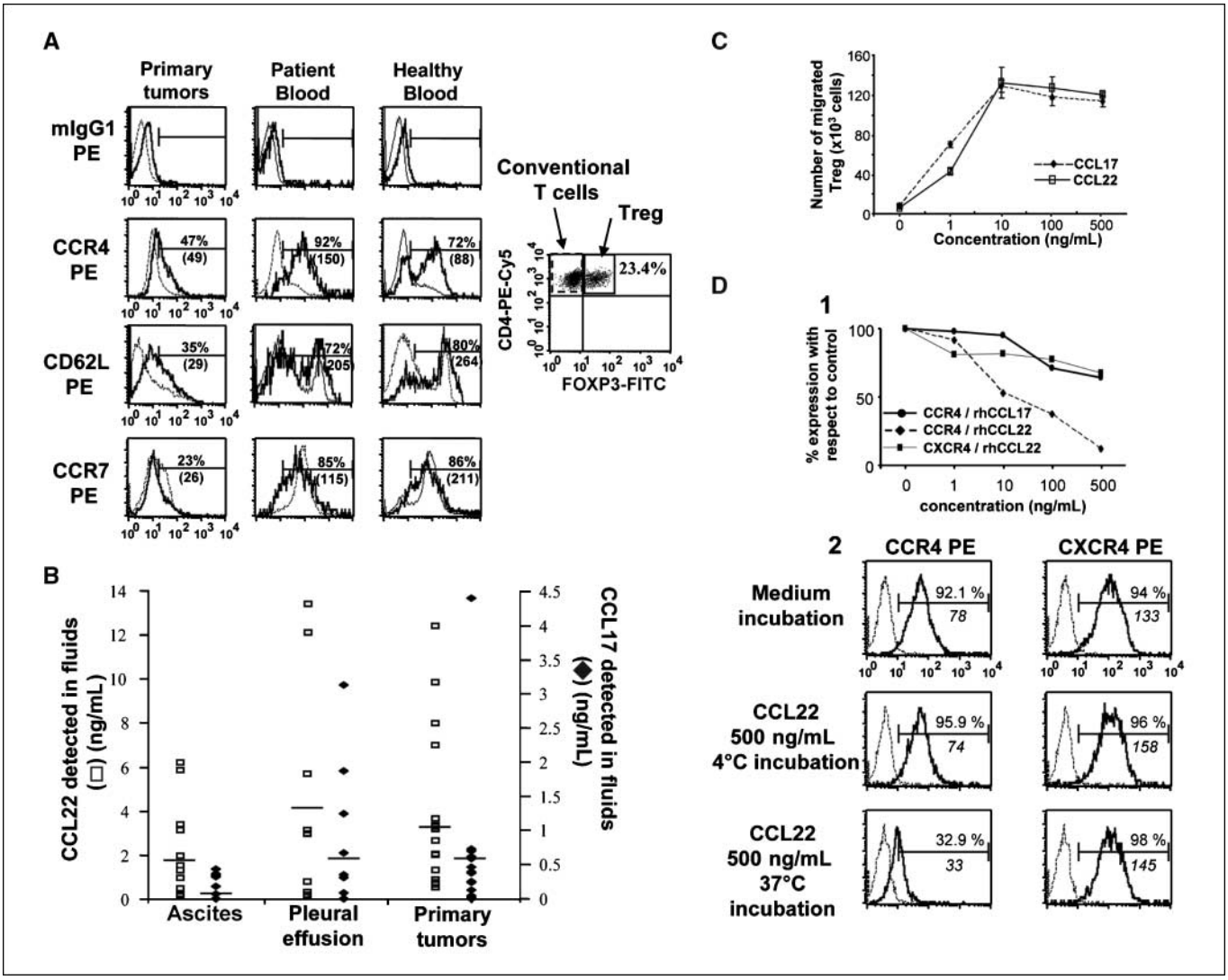

Figure 2. Ti-Treg are selectively recruited in primary tumors probably through CCL22/CCR4. *A,* homing receptor expression on Treg from different compartments was analyzed without purification step after gating on the $CD4^+FOXP3^+$ population (*thick line*) or the $CD4^+FOXP3^-$ Tconv compartment (*dotted line*). IgG1 isotype was used as negative control (IgG2a not shown). Percentages of positive Treg and MFI are given ($n = 7$ experiments). *B,* CCL17 and CCL22 production in tumor conditioned medium [primary tumors ($n = 18$), ascites ($n = 14$), or pleural effusions ($n = 9$)] was analyzed by ELISA and concentrations (ng/mL) of CCL22 (□) and CCL17 (◆) were plotted on the graph (mean value is indicated by —). *C,* the migration capacities of Treg were analyzed toward rising rhCCL17 (-→-) or rhCCL22 (—▫—) concentrations ($n = 3$). *D, 1,* graph represents reduction of CCR4 and CXCR4 expression analyzed on Treg after incubation with rising concentrations of rhCCL22 or rhCCL17; *2,* CCR4 and CXCR4 expression were analyzed on Treg incubated for 1.5 h at 37°C or 4°C in the presence of rhCCL22 (500 ng/mL; MFI values in italic; $n = 3$).

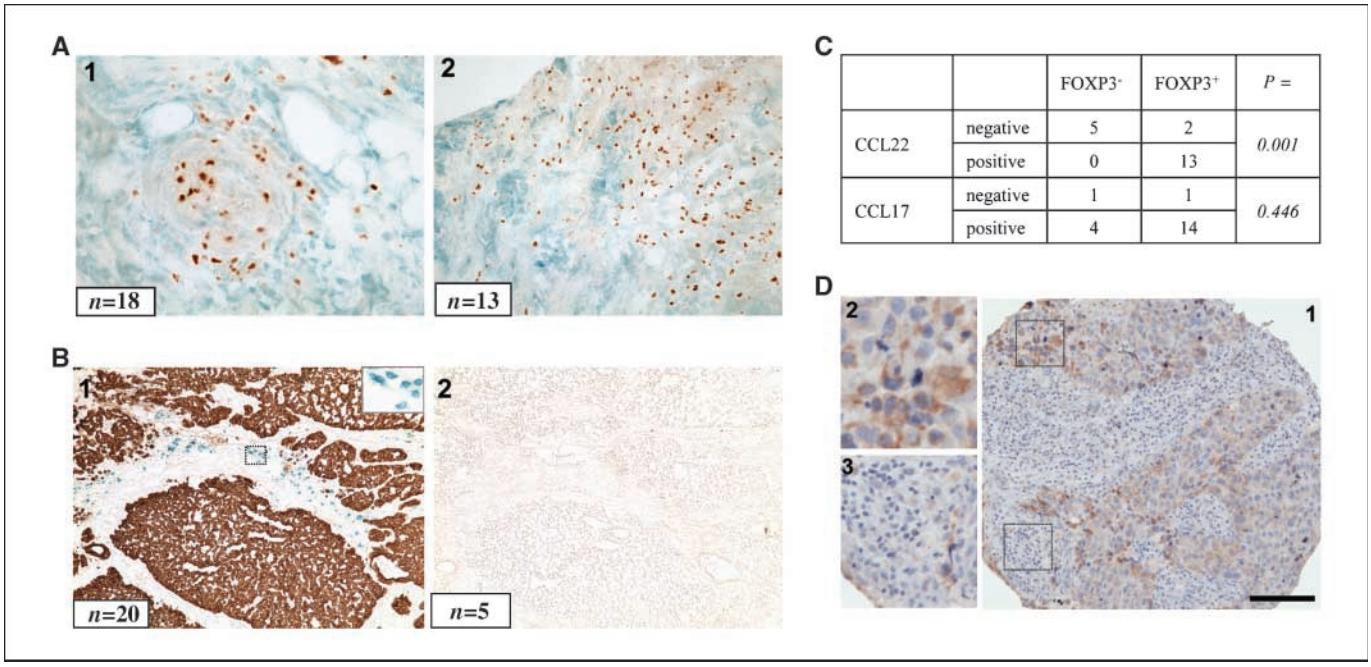

		FOXP3⁻	FOXP3⁺	P =
CCL22	negative	5	2	0.001
	positive	0	13	
CCL17	negative	1	1	0.446
	positive	4	14	

Figure 3. Presence of Ti-Treg was associated with the expression of CCL22 by tumor cells and DC-shaped infiltrating immune cells. *A,* primary breast tumor frozen sections were stained with FOXP3 (*brown*) and CCL17 (magnification, ×20; *1*) or CCL22 (magnification, ×10; *2*) antibodies in green. *B,* sections with cytokeratin$^+$ tumor cells (*brown*) and CD3$^+$ cells (*green*; magnification, ×10; *1*) but lacking CCL22 production (*green*) were not infiltrated by FOXP3$^+$ Ti-Treg (*brown*; magnification, ×10; *2*). Photo magnification in the insert box (×40). *C,* correlation between FOXP3 expression and CCL17 or CCL22 expression on 20 frozen tumors. *D,* paraffin-embedded primary breast tumor sections were stained with CCL22 antibody showing the production of CCL22 by tumor cells (*1* and *2*) but also DC-shaped infiltrating immune cells (*1* and *3*). *Bar,* 100 μm.

observed at 37°C but not at 4°C following incubation with increasing concentrations of rhCCL22 (Fig. 2*D, 1* and *2*) but surprisingly not with rhCCL17 (63% loss of CCR4 staining with 100 ng/mL rhCCL22 versus 7% for rhCCL17; Fig. 2*D, 1*).

CCL22 was detected at high levels either in 48 hours conditioned medium from primary tumor (SN-TUM), ascites, or pleural effusion cell suspensions (Fig. 2*B*) or in metastatic effusions (data not shown). CCL17 was also detectable but at lower levels (Fig. 2*B*). Furthermore, double stainings performed on frozen sections of 20 tumors also showed the production of CCL22 (13 of 20) and CCL17 (18 of 20) by tumor cells (Fig. 3*A, 1* and *2*). A strong correlation was observed between the presence of FOXP3$^+$ Ti-Treg and CCL22 expression by immunohistochemistry (P = 0.001) but not with CCL17 (P = 0.447; Fig. 3*C*). Importantly, although CCL22-negative tumors (5 of 20) did not contain FOXP3$^+$ Ti-Treg (Fig. 3*B, 2*), they were strongly infiltrated by T cells (Fig. 3*B, 1*). CCL22 analyses on paraffin-embedded TMA sections showed that CCL22, which was mainly expressed as a perinuclear staining by tumor cells (Fig. 3*D, 1* and *2*), was also detected within infiltrating immune cells with DC morphology (Fig. 3*D, 1* and *3*). Furthermore, *in vitro* coculture experiments between breast tumor cell lines and PBMC induced high levels of CCL22 that was mainly mediated by monocytes and mDC (data not shown). Of strong interest, CCL22 production strongly correlated with the presence of FOXP3$^+$ Treg in the lymphoid infiltrates (P = 0.008; Supplementary Table S3) but not with the presence of FOXP3$^+$ cells in the tumor bed (P = 0.213).

Altogether, these observations strongly suggest an active recruitment of Treg from the blood to the lymphoid infiltrates surrounding the tumor mass through CCR4 and CCL22 produced in the tumor.

Only Treg within lymphoid aggregates surrounding primary tumors are activated. Treg, whatever their origin, expressed intracytoplasmic CTLA-4 with percentage fluctuation related to sample variability. In contrast to Treg from ascites (Fig. 4) or blood Treg, Ti-Treg expressed high levels of membrane GITR and ICOS, two activation markers, as well as high levels of HLA-DR. Of importance, Tconv cells infiltrating the tumor expressed significantly lower levels of GITR (P = 0.001) and HLA-DR ($P < 10^{-4}$) and almost completely lacked ICOS ($P < 10^{-4}$) expression (Fig. 4; Supplementary Fig. S6). Moreover, higher levels of ICOS and GITR were also observed on healthy blood Treg after *in vitro* stimulation (Supplementary Fig. S2*B*).

These results were strengthened *in situ* on frozen primary breast tumor sections. FOXP3$^+$ cells, which could be observed in contact with CD8$^+$ T cells (Fig. 5*C, 2*), represented a part of CD3$^+$-infiltrating T cells detected in the lymphocyte aggregates (Fig. 5*A, 1* and *2*, and *C, 2*). Importantly, in these infiltrates, all Treg and only Treg coexpressed ICOS (Fig. 5*A, 3*). Furthermore, within tumor cell area cytokeratin$^+$, no ICOS$^+$ Treg were detected (Fig. 5*B, 1*). As shown in Fig. 4 and Supplementary Fig. S6, 5% to 50% of FOXP3$^+$ICOS$^-$ Ti-Treg that did not express other activation markers are detected in tumor dilacerations (data not shown), suggesting that they could represent FOXP3$^+$ Treg observed within the tumor mass.

These results show that Ti-Treg observed within the lymphoid aggregates, but not in the tumor bed of BC, have an activated phenotype.

Ti-Treg proliferate in primary tumors. To evaluate whether Ti-Treg infiltration in tumor results from local proliferation, Ki67 staining was performed both on Ti-Treg and matched peripheral blood Treg without purification step. Ti-Treg (9.88%; range, 7.4–11.7) expressed Ki67 compared with only 4.1% (range, 2.8-5.9) of peripheral blood Treg, strongly suggesting their active *in situ* proliferation (Fig. 6*A* and *B*). Ki67$^+$ cells were also detected to a

lower extent within memory CD4$^+$ Tconv (2.1%; range, 1.87–3). This observation was also further strengthened using Hoechst 33342 that allows the analysis of the DNA cell content (Fig. 6*C*).

The presence of Ki67$^+$ proliferating cells was assessed by double immunostainings on frozen primary breast tumor sections from 10 patients. Besides the Ki67 staining found within the cytokeratin$^+$ tumor cells (Fig. 5*B, 2*), we detected, in the lymphoid area, a subset of ICOS$^+$ Ti-Treg expressing Ki67 (Fig. 5*B, 3*).

Taken together, our results clearly show the presence of proliferating ICOS$^+$ Ti-Treg in primary tumors within lymphoid infiltrates.

Interestingly, the presence of FOXP3$^+$ Treg in the lymphoid infiltrates was strongly correlated to the presence of CD3$^+$ T cells and mature DC (CD208/DC-LAMP$^+$; $P < 10^{-4}$; Supplementary Table S3). Preliminary analyses of the entire T-cell receptor (TCR) repertoire (29) performed on purified Ti-Treg and Tconv from three patients with primary tumor showed that, in contrast to Tconv that have a highly diversified TCR repertoire (40–76.5% combinatorial diversity), Ti-Treg had a skewed TCR repertoire (33–44.4% combinatorial diversity) associated with the emergence of specific rearrangements (up to 7% for 1 TCR and 25% for the 10 major TCR rearrangements; data not shown). This was reinforced by the presence of Ti-Treg close to mature DC-LAMP$^+$ DC within lymphoid infiltrates observed on cryopreserved breast tumor sections (Fig. 5*C, 1*) and strongly suggests the important role of mature DC in the local expansion of tumor-associated antigen (TAA)–specific Ti-Treg.

Discussion

Here, we show, in BC, the presence of Ti-FOXP3$^+$ T cells that are typical Treg based on their CD4$^+$CD25^{high}CD127^{low}FOXP3$^+$ phenotype, their anergic state on *in vitro* stimulation, and their suppressive functions.

The presence of these Ti-Treg within lymphoid infiltrates surrounding the tumor, but not within the tumor itself, is associated to a higher risk of relapse and death, especially in ER$^+$ patients. We provide evidences that this clinical observation could result from the selective recruitment of Treg within lymphoid infiltrates of breast tumors where they are locally activated, likely through TAA recognition, leading to their *in situ* proliferation and prevention of Tconv activation.

The analysis by immunohistochemistry of 191 tumors showed that FOXP3$^+$ cells are present within the tumor area as well as in lymphoid infiltrates. Patients with tumors containing ≥28 FOXP3$^+$ Ti-Treg/spot in lymphoid infiltrates at the periphery of the tumor presented an increased risk of relapse with shorter RFS and OS particularly in the ER$^+$ subgroup, in agreement with previous

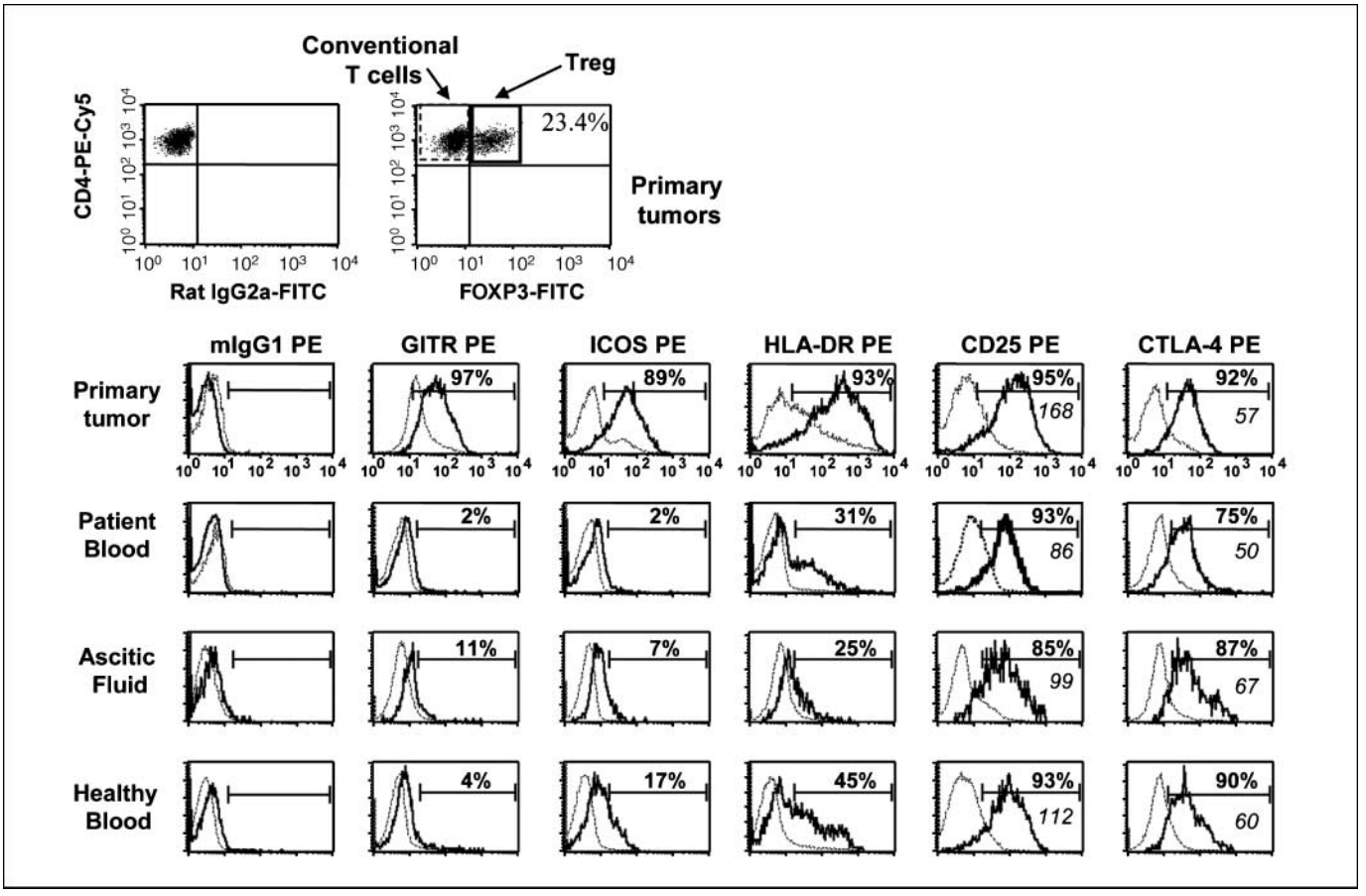

Figure 4. Only Treg cells within breast primary tumor present an activated phenotype. The phenotype of Treg from primary tumors, effusion fluids, patient peripheral blood, and healthy donor blood was compared after triple staining with FOXP3-FITC, CD4-PE-Cy5, and specific antibodies coupled to PE without purification step. Treg activation status was characterized after gating on the CD4$^+$FOXP3$^+$ population (*thick line*) and compared with the CD4$^+$FOXP3$^-$ Tconv compartment (*dotted line*). Cell surface (CD25, GITR, HLA-DR, and ICOS) or intracytoplasmic (CTLA-4 and FOXP3) stainings were performed. Specific isotypes were used as negative control. Results for mouse IgG1 are shown; similar results were obtained for mouse IgG2a (data not shown). For CD25 and CTLA-4 stainings, MFI values are in italic. Results are from a representative experiment.

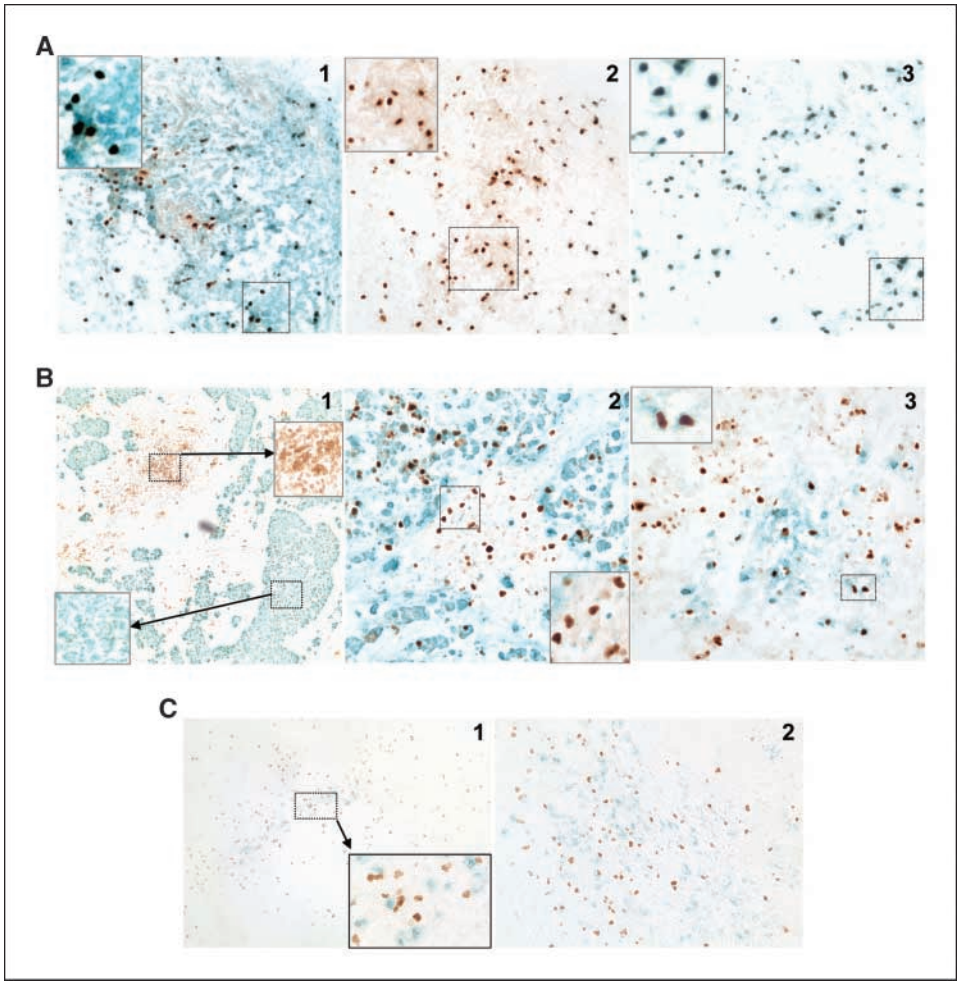

Figure 5. *In situ* analysis of Ti-Treg–expressing ICOS on primary tumor frozen sections. *A,* primary breast tumor frozen sections were double stained with FOXP3 in brown and either CD3 (magnification, ×20; *1*), isotype control (magnification, ×20; *2*), or ICOS (magnification, ×20; 3) in green. *B, 1,* ICOS$^+$ (*brown*) Treg were detectable within lymphoid aggregates (magnification, ×10). Cell proliferation was assessed with Ki67 (*brown*) combined with either cytokeratin (magnification, ×20; *2*) or ICOS (magnification, ×20; *3*) in green. Photo magnification in the insert boxes (×40). *C,* primary breast tumor frozen sections were double stained with FOXP3 in brown and either DC-LAMP (magnification, ×10; magnification in the insert box, ×40; *1*) or CD8 (magnification, ×10; *2*) in green.

reports in breast tumors (20, 21). The effect of FOXP3$^+$ Treg was also increased when the triple-negative tumors were excluded from the analysis of the cohort (data not shown; ref. 26). However, the other studies did not discriminate between Treg from the tumor bed and from lymphoid infiltrates, a feature that our study revealed critical to detect the prognostic value of Treg infiltration as the presence of FOXP3$^+$ Ti-Treg within the tumor area did not affect the patient evolution. Depending on the tumor type, the presence of Treg within the tumor environment has been reported to have positive (17, 18), negative (14, 20), or no effect (19, 30) on patients' survival. But in most of these studies, the suppressive capacity of Ti-Treg was not analyzed. Our results suggest that analyzing the Treg-suppressive capacity and discriminating between Treg from the tumor bed and from lymphoid infiltrates might also be relevant in these other tumors.

Importantly, this suggests that Treg may act by blocking the reactivation of T-cell response within the lymphocyte infiltrates rather than by interfering with their recruitment or the effector function of immune cells in contact with tumor cells.

Therefore, despite the presence of immune cell infiltrate, the immune system is unable to counteract tumor cell growth. We are now providing evidence that this is likely a consequence of the presence of Ti-Treg within these lymphoid infiltrates. Indeed, we show that the proportion of CD4$^+$CD25^{high}FOXP3$^+$ Ti-Treg was much higher in primary tumors than in the peripheral blood and that this population suppressed CD4$^+$ Tconv proliferation and IL-2 and IFN-γ production.

The high number of Ti-Treg present in the breast tumor environment raises the question of their recruitment. Blood Treg have been shown to express high CCR4 levels and to selectively migrate in response to CCR4 ligands produced in the tumor microenvironment (14, 31–34), with an *in vivo* demonstration in ovarian carcinoma of the crucial role of CCL22 in intratumoral Treg recruitment, using a xenograft tumor model in NOD/SCID (14). However, we observed that, in contrast, Ti-Treg expressed very low to undetectable CCR4 levels. Herein, we show that this decreased CCR4 expression could result from its internalization *in vivo* consecutive to an active recruitment, through CCL22, but not CCL17, highly produced by tumor cells, as observed after incubation of blood Treg with CCL22 *in vitro*. This was strengthened by immunohistochemical analyses on cryopreserved tumor sections, which showed a strong correlation between Ti-Treg infiltration and *in situ* CCL22 but not CCL17 tumor expression. Moreover, the implication of CCL22 in recruiting Ti-Treg in lymphoid infiltrates was further expanded by TMA analyses showing that CCL22 produced by tumor cells strongly correlated with the presence of FOXP3$^+$ Ti-Treg in lymphoid infiltrates but not in the tumor area. The decreased expression of CD62L observed on Ti-Treg is also in agreement with an active recruitment as reported in lymph node and gastric carcinoma (31). These observations

suggest, as in lymphoid organs, cooperation between CD62L and CCR4 in the recruitment of Treg from the blood to the lymphoid infiltrates surrounding the tumor. In line with this hypothesis, experiments using Treg from CCR4$^{-/-}$ mice or conditional CCR4 knockout mice in FOXP3$^+$ Treg compartment have recently identified the critical role of CCR4 in Treg trafficking in secondary lymphoid organs (35) or tissues (36). Furthermore, we observed that *in vitro* interaction between myeloid cells (monocytes and DC) and tumor cells leads to increased CCL22 production, suggesting that initial immune cell infiltration elicits the production of CCL22, allowing Treg recruitment within the lymphocyte infiltrates leading to conventional T-cell silencing, in accordance with previous studies showing the high production of CCL22 by mDC (37, 38). These observations identify CCR4/CCL22 as a potential target for therapeutic intervention in BC.

In addition, we showed that, in contrast to paired blood Treg, Ti-Treg display an activated phenotype, as they expressed high levels of membrane GITR and ICOS. Of note, expression of ICOS and GITR was up-regulated on healthy blood Treg following *in vitro* TCR activation (Supplementary Fig. S2; ref. 23). In the past 5 years, ICOS costimulation has been largely implicated in the induction of regulatory cell-mediated tolerance and the production of IL-10 (39–42). More recently, it has been shown that the ICOS$^+$FOXP3$^+$ Treg population suppressed DC and T-cell functions through IL-10 and transforming growth factor-β,respectively, and that stimulation with ICOS-L promotes their survival and proliferation (43).

Whereas only 30% of Treg expressed low levels of HLA-DR in patient peripheral blood, all Ti-Treg highly expressed HLA-DR, previously described to identify, in humans, a mature Treg population expressing high FOXP3 levels and exerting functionally distinct contact-dependent suppression (44). The present observation in BC is in marked contrast with results observed in lymph nodes from melanoma and non–Hodgkin's lymphoma where Treg displayed low levels of HLA-DR expression as in paired peripheral blood (34, 45), thus suggesting that the primary tumor environment plays an active role in the induction of HLA-DR on breast Ti-Treg.

Moreover, in contrast to peripheral blood Treg, a consistent part of Ti-Treg proliferates *in situ* as shown by flow cytometry with Ki67 expression and Hoechst 33342 incorporation. This is consistent with the observation that Treg from cancer patients, including BC, exhibit significantly decreased levels of TREC when compared with Treg from healthy controls (46).

Importantly, the CD4$^+$ Tconv cell counterpart in primary tumors expressed low GITR levels and did neither express ICOS, nor MHC class II, nor proliferate.

Taken together, the activated phenotype of Ti-Treg (GITR^{high}ICOS$^+$HLA-DR$^+$) observed in BC primary tumors strongly suggests an *in situ* activation in response to TAA and local immunosup-

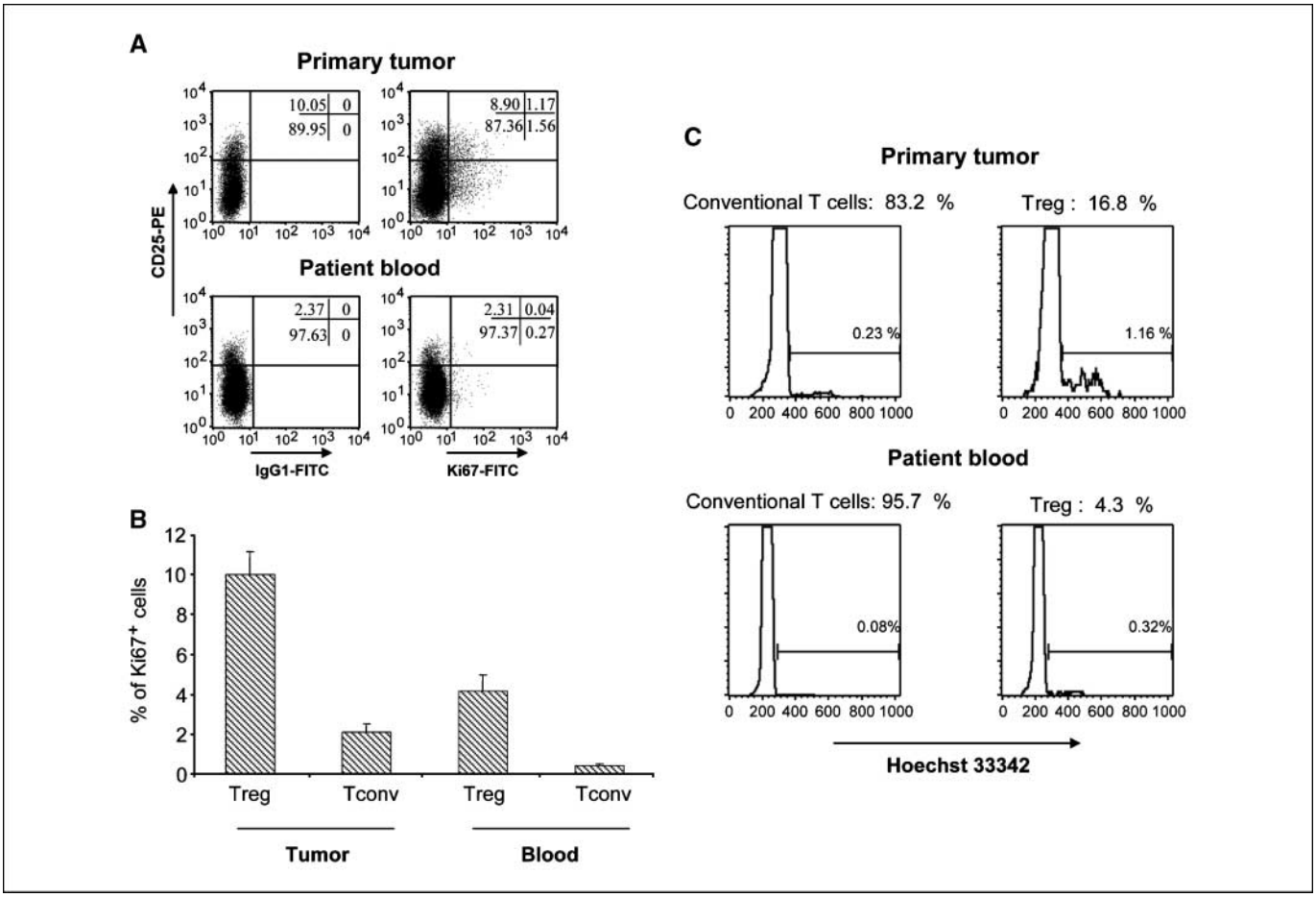

Figure 6. CD4$^+$CD25^{high}FOXP3$^+$ T cells proliferate within the tumor area. *A* and *B, in situ* proliferation of Treg from primary tumor and matched peripheral blood was assessed without purification step. Triple staining with Ki67-FITC, CD25-PE, and CD4-PE-Cy5 was performed. *A,* dot plots gated on CD4$^+$ cells obtained in the primary tumor and blood from a representative patient. *B, columns,* mean of Ki67$^+$ cells within the Treg or Tconv subsets in tumor and associated blood from five different patients; *bars,* SD. *C,* the percentage of CD4$^+$ Tconv and Treg within cell cycle in patient blood or tumor was analyzed on FACSVantage SE after Hoechst 33342 incorporation (n = 4).

pressive functions that dominate the tumor environment, leading to prevention of Tconv cell activation, as illustrated by the resting state of $CD8^+$ T cells present in the vicinity of Ti-Treg, within lymphoid aggregates.

Furthermore, by immunohistochemical staining, we showed the presence of $Ki67^+$ among Ti-Treg that all express ICOS within lymphoid aggregates, whereas Treg within tumor bed are all negative. As quantified by flow cytometry, the ICOS-negative Treg subset, variable in frequency from patient to patient (5–50%), never expressed other activation markers. This shows that Ti-Treg are selectively activated within lymphoid infiltrates where they exert their suppressive function as suggested by their effect on clinical outcome. In this context, mature DC could allow the expansion of Treg (47, 48) and are only present within the lymphoid infiltrates (6, 9), where their detection by DC-LAMP staining was strongly correlated with the presence of $FOXP3^+$ Treg.

In conclusion, our results show for the first time that, in BC, Treg are actively recruited within lymphoid infiltrates, probably through CCR4/CCL22. Our observations further allow to propose that Ti-Treg are selectively activated ($CD45RO^+GITR^+ICOS^+HLA\text{-}DR^+$) within lymphoid infiltrates possibly through TAA presentation by mature DC (colocalization of DC-$LAMP^+$ and $FOXP3^+$), resulting in their local expansion ($Ki67^+$, Hoechst 33342 staining, and skewed TCR repertoire) and Tconv cell suppression and ultimately tumor progression and patient relapse.

This study validates Treg neutralization as a crucial therapeutic objective to improve immunotherapy and identifies CCR4/CCL22 and ICOS as potential therapeutic targets in breast tumors that represents, in Western countries, a major health problem.

Disclosure of Potential Conflicts of Interest

No potential conflicts of interest were disclosed.

Acknowledgments

Received 6/20/2008; revised 12/9/2008; accepted 12/23/2008; published OnlineFirst 02/24/2009.

Grant support: The Breast Cancer Research Foundation, Ligue Nationale Contre le Cancer (Lig69), Institut National du Cancer (CANCEROPOLE 2004-05, INCa ACI-63-04, and "METESCAPE"), and ARC (ARC-3364). M. Gobert is a grant holder of the ANRT with financial support of the Centre Léon Bérard. For his last Ph.D. year, he is financed by the Ligue Contre le Cancer (Lig69).

The costs of publication of this article were defrayed in part by the payment of page charges. This article must therefore be hereby marked *advertisement* in accordance with 18 U.S.C. Section 1734 solely to indicate this fact.

We thank the BC patients who consented to participate in this study; X.N. N'Guyen, G. Poyet, and C. Rigal for technical support; and M.D. Reynaud for critical reading of the manuscript.

References

1. Dunn GP, Old LJ, Schreiber RD. The immunobiology of cancer immunosurveillance and immunoediting. Immunity 2004;21:137–48.
2. Menetrier-Caux C, Bain C, Favrot MC, Duc A, Blay JY. Renal cell carcinoma induces interleukin 10 and prostaglandin E2 production by monocytes. Br J Cancer 1999;79:119–30.
3. Menetrier-Caux C, Montmain G, Dieu MC, et al. Inhibition of the differentiation of dendritic cells from CD34(+) progenitors by tumor cells: role of interleukin-6 and macrophage colony-stimulating factor. Blood 1998; 92:4778–91.
4. Thomachot MC, Bendriss-Vermare N, Massacrier C, et al. Breast carcinoma cells promote the differentiation of CD34+ progenitors towards 2 different subpopulations of dendritic cells with CD1a(high)CD86(−)Langerin− and CD1a(+)CD86(+)Langerin+ phenotypes. Int J Cancer 2004;110:710–20.
5. Zou W. Regulatory T cells, tumour immunity and immunotherapy. Nat Rev Immunol 2006;6:295–307.
6. Bell D, Chomarat P, Broyles D, et al. In breast carcinoma tissue, immature dendritic cells reside within the tumor, whereas mature dendritic cells are located in peritumoral areas. J Exp Med 1999;190:1417–26.
7. Ben Hur H, Cohen O, Schneider D, et al. The role of lymphocytes and macrophages in human breast tumorigenesis: an immunohistochemical and morphometric study. Anticancer Res 2002;22:1231–8.
8. Beckhove P, Feuerer M, Dolenc M, et al. Specifically activated memory T cell subsets from cancer patients recognize and reject xenotransplanted autologous tumors. J Clin Invest 2004;114:67–76.
9. Treilleux I, Blay JY, Bendriss-Vermare N, et al. Dendritic cell infiltration and prognosis of early stage breast cancer. Clin Cancer Res 2004;10:7466–74.
10. Liu YJ. IPC: professional type 1 interferon-producing cells and plasmacytoid dendritic cell precursors. Annu Rev Immunol 2005;23:275–306.
11. Liyanage UK, Moore TT, Joo HG, et al. Prevalence of regulatory T cells is increased in peripheral blood and tumor microenvironment of patients with pancreas or breast adenocarcinoma. J Immunol 2002;169:2756–61.
12. Perez SA, Karamouzis MV, Skarlos DV, et al. CD4+CD25+ regulatory T-cell frequency in HER-2/neu (HER)-positive and HER-negative advanced-stage breast cancer patients. Clin Cancer Res 2007;13:2714–21.
13. Wolf AM, Wolf D, Steurer M, Gastl G, Gunsilius E, Grubeck-Loebenstein B. Increase of regulatory T cells in the peripheral blood of cancer patients. Clin Cancer Res 2003;9:606–12.
14. Curiel TJ, Coukos G, Zou L, et al. Specific recruitment of regulatory T cells in ovarian carcinoma fosters immune privilege and predicts reduced survival. Nat Med 2004;10:942–9.
15. Hiraoka N, Onozato K, Kosuge T, Hirohashi S. Prevalence of FOXP3+ regulatory T cells increases during the progression of pancreatic ductal adenocarcinoma and its premalignant lesions. Clin Cancer Res 2006;12:5423–34.
16. Kobayashi N, Hiraoka N, Yamagami W, et al. FOXP3+ regulatory T cells affect the development and progression of hepatocarcinogenesis. Clin Cancer Res 2007;13: 902–11.
17. Carreras J, Lopez-Guillermo A, Fox BC, et al. High numbers of tumor-infiltrating FOXP3-positive regulatory T cells are associated with improved overall survival in follicular lymphoma. Blood 2006;108:2957–64.
18. Badoual C, Hans S, Rodriguez J, et al. Prognostic value of tumor-infiltrating CD4+ T-cell subpopulations in head and neck cancers. Clin Cancer Res 2006;12: 465–72.
19. Grabenbauer GG, Lahmer G, Distel L, Niedobitek G. Tumor-infiltrating cytotoxic T cells but not regulatory T cells predict outcome in anal squamous cell carcinoma. Clin Cancer Res 2006;12:3355–60.
20. Bates GJ, Fox SB, Han C, et al. Quantification of regulatory T cells enables the identification of high-risk breast cancer patients and those at risk of late relapse. J Clin Oncol 2006;24:5373–80.
21. Bohling SD, Allison KH. Immunosuppressive regulatory T cells are associated with aggressive breast cancer phenotypes: a potential therapeutic target. Mod Pathol 2008;21:1527–32.
22. Morelle M, Hasle E, Treilleux I, et al. Cost-effectiveness analysis of strategies for HER2 testing of breast cancer patients in France. Int J Technol Assess Health Care 2006;22:396–401.
23. Hoffmann P, Eder R, Kunz-Schughart LA, Andreesen R, Edinger M. Large-scale *in vitro* expansion of polyclonal human CD4(+)CD25high regulatory T cells. Blood 2004;104:895–903.
24. Vanbervliet B, Bendriss-Vermare N, Massacrier C, et al. The inducible CXCR3 ligands control plasmacytoid dendritic cell responsiveness to the constitutive chemokine stromal cell-derived factor 1 (SDF-1)/CXCL12. J Exp Med 2003;198:823–30.
25. Pruthi S, Brandt KR, Degnim AC, et al. A multidisciplinary approach to the management of breast cancer, part 1: prevention and diagnosis. Mayo Clin Proc 2007; 82:999–1012.
26. Banerjee S, Reis-Filho JS, Ashley S, et al. Basal-like breast carcinomas: clinical outcome and response to chemotherapy. J Clin Pathol 2006;59:729–35.
27. Banham AH. Cell-surface IL-7 receptor expression facilitates the purification of FOXP3(+) regulatory T cells. Trends Immunol 2006;27:541–4.
28. Imai T, Chantry D, Raport CJ, et al. Macrophage-derived chemokine is a functional ligand for the CC chemokine receptor 4. J Biol Chem 1998;273:1764–8.
29. Pasqual N, Gallagher M, Aude-Garcia C, et al. Quantitative and qualitative changes in V-J α rearrangements during mouse thymocytes differentiation: implication for a limited T cell receptor α chain repertoire. J Exp Med 2002;196:1163–73.
30. Siddiqui SA, Frigola X, Bonne-Annee S, et al. Tumor-infiltrating Foxp3-4+CD25+ T cells predict poor survival in renal cell carcinoma. Clin Cancer Res 2007;13: 2075–81.
31. Enarsson K, Lundgren A, Kindlund B, et al. Function and recruitment of mucosal regulatory T cells in human chronic *Helicobacter pylori* infection and gastric adenocarcinoma. Clin Immunol 2006;121:358–68.
32. Ishida T, Ishii T, Inagaki A, et al. Specific recruitment of CC chemokine receptor 4-positive regulatory T cells in Hodgkin lymphoma fosters immune privilege. Cancer Res 2006;66:5716–22.
33. Miller AM, Lundberg K, Ozenci V, et al. CD4+CD25high T cells are enriched in the tumor and peripheral blood of prostate cancer patients. J Immunol 2006;177:7398–405.
34. Yang ZZ, Novak AJ, Stenson MJ, Witzig TE, Ansell SM. Intratumoral CD4+CD25+ regulatory T-cell-mediated suppression of infiltrating CD4+ T cells in B-cell non-Hodgkin lymphoma. Blood 2006;107:3639–46.
35. Yuan Q, Bromley SK, Means TK, et al. CCR4-dependent regulatory T cell function in inflammatory bowel disease. J Exp Med 2007;204:1327–34.
36. Sather BD, Treuting P, Perdue N, et al. Altering the distribution of Foxp3(+) regulatory T cells results in tissue-specific inflammatory disease. J Exp Med 2007; 204:1335–47.
37. Godiska R, Chantry D, Raport CJ, et al. Human

macrophage-derived chemokine (MDC) a novel chemoattractant for monocytes monocyte-derived dendritic cells and natural killer cells. J Exp Med 1997;185:1595–604.
38. Vulcano M, Albanesi C, Stoppacciaro A, et al. Dendritic cells as a major source of macrophage-derived chemokine/CCL22 *in vitro* and *in vivo*. Eur J Immunol 2001;31:812–22.
39. Akbari O, Freeman GJ, Meyer EH, et al. Antigen-specific regulatory T cells develop via the ICOS-ICOS-ligand pathway and inhibit allergen-induced airway hyperreactivity. Nat Med 2002;8:1024–32.
40. Herman AE, Freeman GJ, Mathis D, Benoist C. CD4+CD25+ T regulatory cells dependent on ICOS promote regulation of effector cells in the prediabetic lesion. J Exp Med 2004;199:1479–89.
41. Kohyama M, Sugahara D, Sugiyama S, Yagita H, Okumura K, Hozumi N. Inducible costimulator-dependent IL-10 production by regulatory T cells specific for self-antigen. Proc Natl Acad Sci U S A 2004;101:4192–7.
42. Vermeiren J, Ceuppens JL, Van Ghelue M, et al. Human T cell activation by costimulatory signal-deficient allogeneic cells induces inducible costimulator-expressing anergic T cells with regulatory cell activity. J Immunol 2004;172:5371–8.
43. Ito T, Hanabuchi S, Wang YH, et al. Two functional subsets of FOXP3(+) regulatory T cells in human thymus and periphery. Immunity 2008;28:870–80.
44. Baecher-Allan C, Wolf E, Hafler DA. MHC class II expression identifies functionally distinct human regulatory T cells. J Immunol 2006;176:4622–31.
45. Viguier M, Lemaitre F, Verola O, et al. Foxp3 expressing CD4+CD25(high) regulatory T cells are overrepresented in human metastatic melanoma lymph nodes and inhibit the function of infiltrating T cells. J Immunol 2004;173:1444–53.
46. Wolf D, Rumpold H, Koppelstatter C, et al. Telomere length of *in vivo* expanded CD4(+)CD25 (+) regulatory T-cells is preserved in cancer patients. Cancer Immunol Immunother 2006;55:1198–208.
47. Kubo T, Hatton RD, Oliver J, Liu X, Elson CO, Weaver CT. Regulatory T cell suppression and anergy are differentially regulated by proinflammatory cytokines produced by TLR-activated dendritic cells. J Immunol 2004;173:7249–58.
48. Yamazaki S, Iyoda T, Tarbell K, et al. Direct expansion of functional CD25+ CD4+ regulatory T cells by antigen-processing dendritic cells. J Exp Med 2003;198:235–47.